AIAA JOURNAL
Vol. 33, No. 5, May 1995

Linear Stability of Differentially Heated Spatially Developing Layers

Omar M. Knio* and Xiyan Shi†
Johns Hopkins University, Baltimore, Maryland 21218

Heterogeneous shear layers, characterized by the presence of a wake deficit and a Gaussian temperature profile, are considered. Unstable mode characteristics are interpreted in terms of a five-parameter set which describes the velocity ratio and the thicknesses and strengths of the wake component and temperature spike. In the absence of a wake deficit, the Kelvin–Helmholtz mode is inhibited as density gradients increase. Stabilization of this mode is weak (strong) when the density profile thickness is larger (smaller) than that of the shear layer. When a wake component is present, stabilization of the Kelvin–Helmholtz instability is no longer observed. In this case, the growth rate of unstable Kelvin–Helmholtz waves is found to be weakly sensitive to the presence of a heated region and to the details of the wake deficit.

I. Introduction

THE stability properties of heterogeneous free shear flows may be strongly dependent on the prevailing density distribution. For instance, it has long been observed that a nonunity density ratio may significantly alter the early growth of free shear layers and even modulate the vortical structures which form at later stages of evolution.[1–6] The presence of zones of large density variation may also affect the nature of dominant flow instabilities. Theoretical and experimental results on heated jets provide dramatic illustrations of the impact of density variations on global flow features, especially when these cause a transition from convectively to absolutely unstable fields.[7–10] The stability of reacting shear flows also appears to exhibit a strong sensitivity to the prevailing density distribution which, in this case, is governed by heat release mechanisms. Recent studies indicate that, depending on the configuration of velocity and density distributions, flowfield stabilization or destabilization may occur.[11–16]

Linear stability predictions were successful in providing fundamental interpretation of the observed behavior of a large number of heterogeneous free shear flows. Unfortunately, application of linear stability analysis to characterize the properties of reacting shear flow often suffers from the extreme sensitivity of the results to assumed velocity and density profiles.[11] To overcome this difficulty, Shin and Ferziger[12] have emphasized the use of "correct" initial conditions. Thus, in their analysis of nonpremixed reacting shear layers, a boundary-layer solution of a laminar reacting flow problem is first obtained which is initially given by a velocity discontinuity between equal-density oxidizer and fuel streams. The resulting density profile and monotonic velocity distribution are then used as initial conditions for the stability problem. In particular, their analysis reveals that stabilization of Kelvin–Helmholtz modes occurs as the density within the layer decreases due to heat release (see also Jackson and Grosch[10] and Hu et al.[11]).

The modeling of shear layers using a monotonic velocity profile—whether experimentally fitted using a similarity variable or analytically determined starting with an initial discontinuity—does not always constitute a valid approach. This issue has been addressed by Koochesfahani and Frieler[1] who analyzed the spatial instability of shear layers at high density ratio. In this study, the shear layer resulting from the merger of unequal boundary layers is modeled by superposing a wake component on the experimentally fitted monotonic shear layer profile. By doing so, the analysis indicates that when the density of the low-speed stream is much larger than that of the high-speed stream, the unstable wake mode becomes dominant. These findings are in agreement with experimental observations which show that under these conditions the formation of wake vortices replaces the familiar shedding of Kelvin–Helmholtz eddies.

Motivated in part by the findings of Koochesfahani and Frieler,[1] Knio and Ghoniem[17] considered both monotonic and nonmonotonic velocity profiles in their stability analysis of temporal reacting layers. Selection of these initial conditions was also motivated by experimental observations (e.g. Refs. 18 and 19) which indicate that opposite signs of vorticity may coexist in essentially two-dimensional, homogeneous flow even for large distances downstream of very thin splitter plates. Thus, the establishment of a monotonic velocity profile may not always occur prior to the substantial growth of unstable modes, especially if high-perturbation levels are experienced. Among the important results of the study discussed in Ref. 17 is that the presence of a wake component renders temporal Kelvin–Helmholtz modes weakly sensitive to the details of the density distribution. In particular, stabilization of nonmonotonic layers due to heat release is not observed.

One of the limitations of the study performed in Ref. 17 is that only temporal layers were considered. Thus, the objective of this effort is to generalize previous results and to contrast the responses of temporal and spatial layers to the imposed mode of heating. The adopted approach calls for the application of a straightforward stability analysis (Sec. II) to a large set of initial velocity and density profiles (Sec. III). The results of the analysis are given in Sec. IV; major conclusions are summarized in Sec. V.

II. Formulation

We focus our attention on the behavior of small two-dimensional perturbations of spatially developing heterogeneous shear flow in the limits of high Reynolds and Peclet numbers and low Mach and Richardson numbers. The initial flowfield is given in terms of an unbounded parallel shear flow profile $U(y)$ and a density profile, $\rho(y)$, which is assumed to be the result of heat deposition by a nonpremixed reaction front. Under the stated assumptions diffusive phenomena and gravity effects[6] may be ignored, so that the evolution of two-dimensional perturbations is governed by the Rayleigh equation,[1,12,17]

$$\hat{v}'' = -\frac{\rho'}{\rho}\hat{v}' + \left(\frac{U''}{U-\beta/\alpha} + \frac{\rho'}{\rho}\frac{U'}{U-\beta/\alpha} + \alpha^2\right)\hat{v} \qquad (1)$$

written in Eq. (1) in terms of the perturbation cross-stream velocity,

$$v(x, y, t) = \hat{v}(y)\exp[i(\alpha x - \beta t)] \qquad (2)$$

Received Feb. 17, 1994; revision received May 26, 1994; accepted for publication June 11, 1994.

*Assistant Professor, Department of Mechanical Engineering. Member AIAA.
†Graduate Research Assistant, Department of Mechanical Engineering.

where primed quantities denote differentiation with respect to y, $\alpha = \alpha_r + i\alpha_i$ is the complex wave number and β is the frequency. Equations (1) and (2) are accompanied by the far-field boundary conditions, $\hat{v}(y \to \pm\infty) \sim \exp(\mp\alpha y)$, resulting in an eigenvalue problem which is solved numerically. For real frequencies β, Eq. (1) is integrated from both sides of the layer toward $y = 0$, and iterations are performed in the complex eigenvalue space α to ensure that both branches meet at $y = 0$ with equal derivatives.[1,17,20]

III. Initial Conditions

Selection of initial conditions is motivated by a desire to capture the early growth of a reacting spatially developing mixing layer (Fig. 1). Ideally, flowfield configurations used in the stability analysis would closely approximate physical profiles. Unfortunately, the latter are function of a large number of physical parameters. Specifically, the velocity profile downstream of the splitter plate depends on the thicknesses of the splitter plate and upstream boundary layers; the early evolution of the velocity distribution also depends on these parameters as well as the prevailing Reynolds number. Additionally, the early formation of a heated products zone also depends on a large number of physical quantities. In the simplest case, the local structure of the heated zone is a nontrivial function of "inlet" and freestream conditions, the heat of reaction, and Reynolds, Peclet, Lewis, Damkohler, and Zeldovich numbers.[10] Thus, to avoid performing stability calculations in a large parameter space, a simplified flow model is first developed.

In modeling the flowfield, attention is first focused on the impact of heat release. This aspect has already been addressed by Shin and

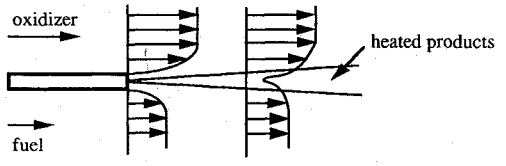

Fig. 1 Schematic illustration of the spatial development of a reacting mixing layer.

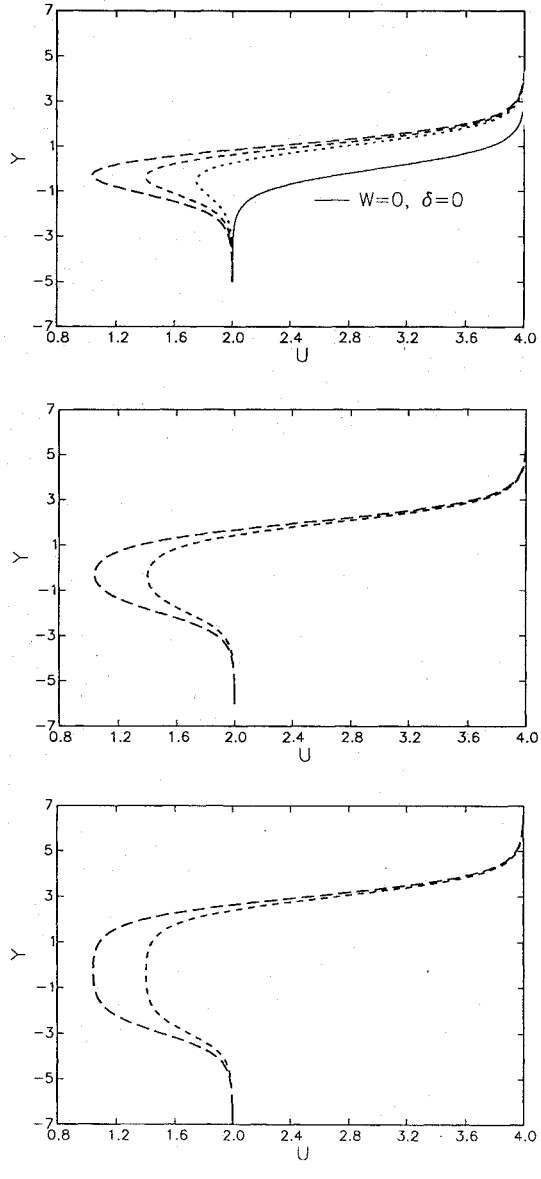

Fig. 2 Shear layer profiles generated using Eq. (4) with $r = \frac{1}{2}$: a) $\delta = 1$, $W = 0.25(\cdots)$, $0.5(- -)$, and $0.75(- -)$, also tanh profile (solid); b) $\delta = 2$, $W = 0.3219(- -)$ and $0.5123(- -)$; and c) $\delta = 3$, $W = 0.3016(- -)$ and $0.4849(- -)$.

Table 1 Velocity profile parameters, $r = \frac{1}{2}$

$\delta = 1$	$W = 0.25$	$W = 0.5$	$W = 0.75$
$\delta = 2$		$W = 0.3219$	$W = 0.5123$
$\delta = 3$		$W = 0.3016$	$W = 0.4849$

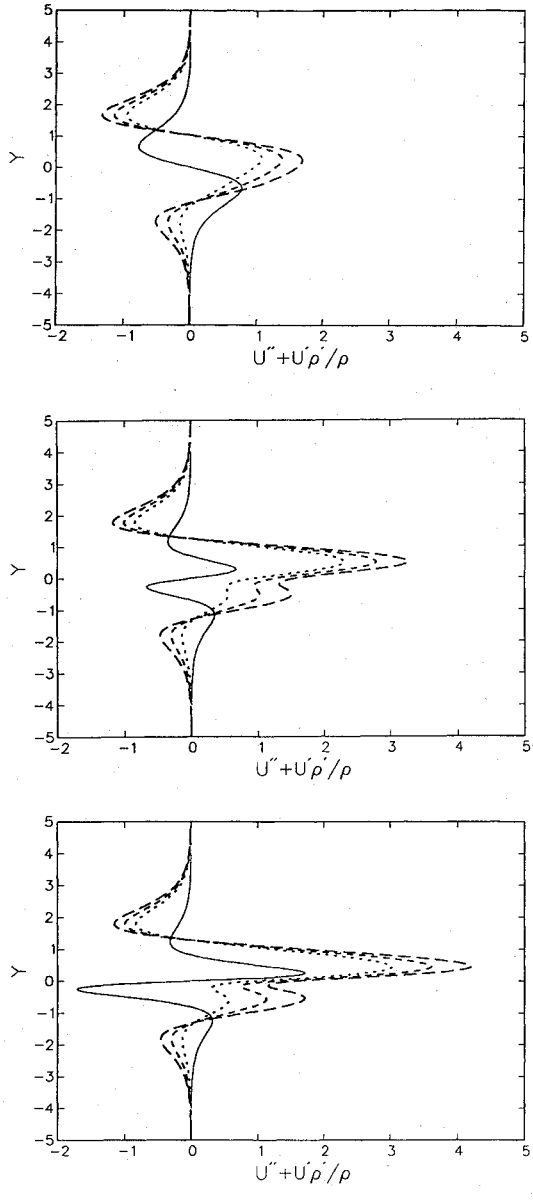

Fig. 3 Profiles of $U'' + \rho' U'/\rho$ corresponding to the velocity profiles of Fig. 2a and density profiles having $\sigma = 1$: a) $T_r = 1$, b) $T_r = 4$, and c) $T_r = 8$.

Ferziger[12] who showed that, for most situations of interest, the evolution of the nonpremixed reaction occurs at a significantly slower rate than the linear growth of unstable modes, at least once a finite thickness product zone has formed. Thus, for the purpose of characterizing the stability properties of the flow, only density variation needs be accounted for; this result justifies our use of the Rayleigh equation (Sec. II). In this study, it is further assumed that the contributing streams have equal density and temperature and obey the perfect gas law. The latter is normalized using the density and temperature of the freestreams so that $\rho T = 1$. Next, the effect of heat release is modeled using a Gaussian temperature spike, specified in terms of its standard deviation σ and by T_r the ratio of the maximum temperature within the layer to the freestream temperature. Thus, the normalized initial density distribution is expressed as

$$\rho(y) = 1 - [(T_r - 1)/T_r]\exp(-y^2/\sigma^2) \tag{3}$$

As mentioned in the Introduction, the modeling of the velocity distribution aims at capturing both the early laminar growth of the layer which is characterized by the presence of a wake deficit and its structure at large downstream distance. To do so, we start with the experimentally fitted similarity profile for a monotonic layer,

$$U(y) = U_m + (\Delta U/2)\tanh(y/\delta_\omega) \tag{4}$$

where $U_m = (U_1 + U_2)/2$ is the mean flow velocity, $\Delta U = U_1 - U_2$ is the velocity difference across the layer, and δ_ω is the local vorticity thickness. In the remainder of this study, $\Delta U/2$ and δ_ω are chosen as characteristic velocity and length scales, respectively. Following Koch,[21] the normalized shear layer profile is then generalized to a larger family of velocity profiles using the expression

$$U(y) = (1 + W)\tanh(y - \delta) - W\tanh(y + \delta) + \gamma \tag{5}$$

where $\gamma \equiv (1 + r)/(1 - r)$ is the normalized mean velocity, $r = U_2/U_1$ is the velocity ratio, W is the wake deficit, and δ is the thickness of the profile. For $W = \delta = 0$ the tanh profile is recovered. When $W < 0$, the resulting velocity profiles model an asymmetric near wake for large δ, and the merger of two Blasius profiles for small δ.

Note that, in most applications, the density profile thickness is smaller than the velocity profile width, $\sigma \leq 1$. However, to account for situations where molecular mixing occurs at a different rate than momentum diffusion, σ is treated as an independent parameter. Furthermore, we note that the wake deficit W is, in general, related to the profile width δ; however, the relationship is not unique since it must depend on the thickness of the initial boundary-layer profiles and of the splitter plate. Thus, to cover a wide range of possibilities, W and δ are also treated as independent parameters.

IV. Results

The spatial stability characteristics of the flowfield are determined in the five-dimensional parameter space $(W, \delta, T_r, \sigma, r)$. We consider a single value of the velocity ratio, $r = \frac{1}{2}$, and three values of the temperature ratio, $T_r = 1$, 4, and 8. The effect of wake deficit is investigated by varying the W and δ simultaneously, so that shear flows having the same velocity maximums and minimums but different profile thickness are obtained (Table 1, Fig. 2). The impact of the heated zone thickness is analyzed by varying σ independently; four values $\sigma = 0.5$, 0.75, 1, and 1.5 are selected in the analysis.

The search for unstable eigenfunctions is guided by theoretical considerations concerning the expected number of unstable modes[12,17] and the long-wave behavior of unstable time-evolving waves.[17,22–25] Briefly, the expected number of unstable waves is determined by inspection of the zeros of the function $U'' + \rho' U'/\rho$. The latter is plotted in Fig. 3 for the profiles of Fig. 2a. The figure shows that when $W \neq 0$, $U'' + \rho' U'/\rho$ admits two zeros, thus, leading us to expect two unstable modes. These are distinguished based on their long-wave asymptotic behavior[17,23]; in the present case, they are unambiguously identified with the Kelvin–Helmholtz and wake modes. Only one zero is detected for the monotonic tanh profile at $T_r = 1$, so that only the Kelvin–Helmholtz mode is expected. On the other hand, three zeros are detected for the tanh

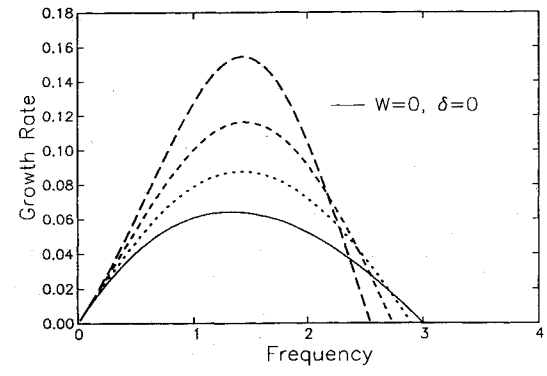

a) K–H mode

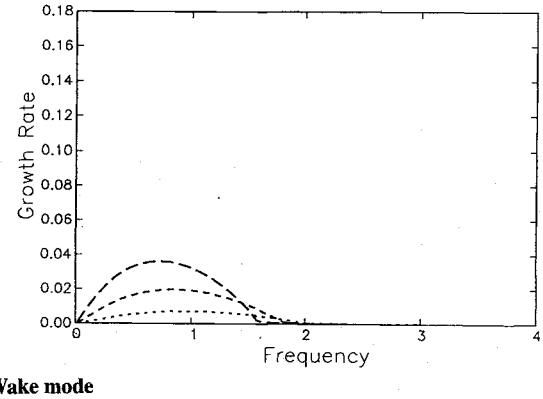

b) Wake mode

Fig. 4 Growth rate vs frequency for a) the Kelvin–Helmholtz mode and b) the wake mode, corresponding to the velocity profiles of Fig. 2a and a homogeneous field $T_r = 1$; results for the tanh profile are shown using a solid line.

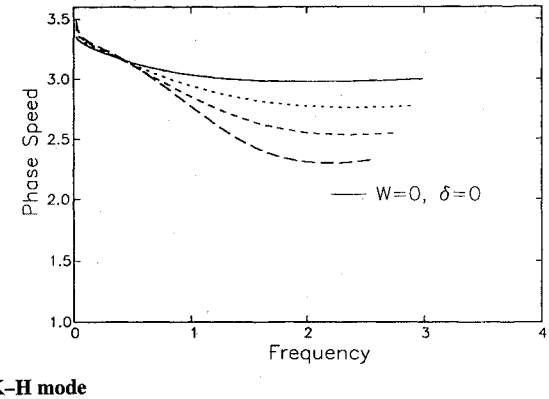

a) K–H mode

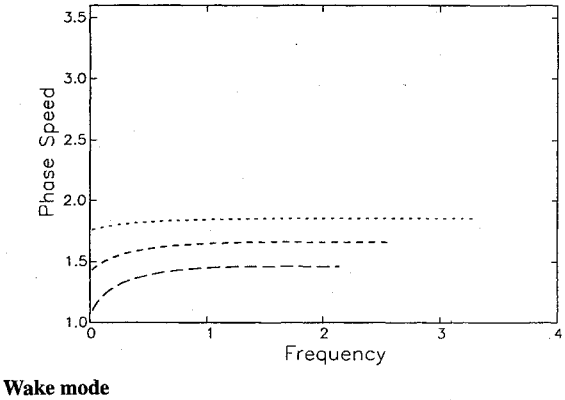

b) Wake mode

Fig. 5 Phase speed vs frequency for a) Kelvin–Helmholtz mode and b) the wake mode, corresponding to the velocity profiles of Fig. 2a and a homogeneous field $T_r = 1$; results for the tanh profile are shown using a solid line.

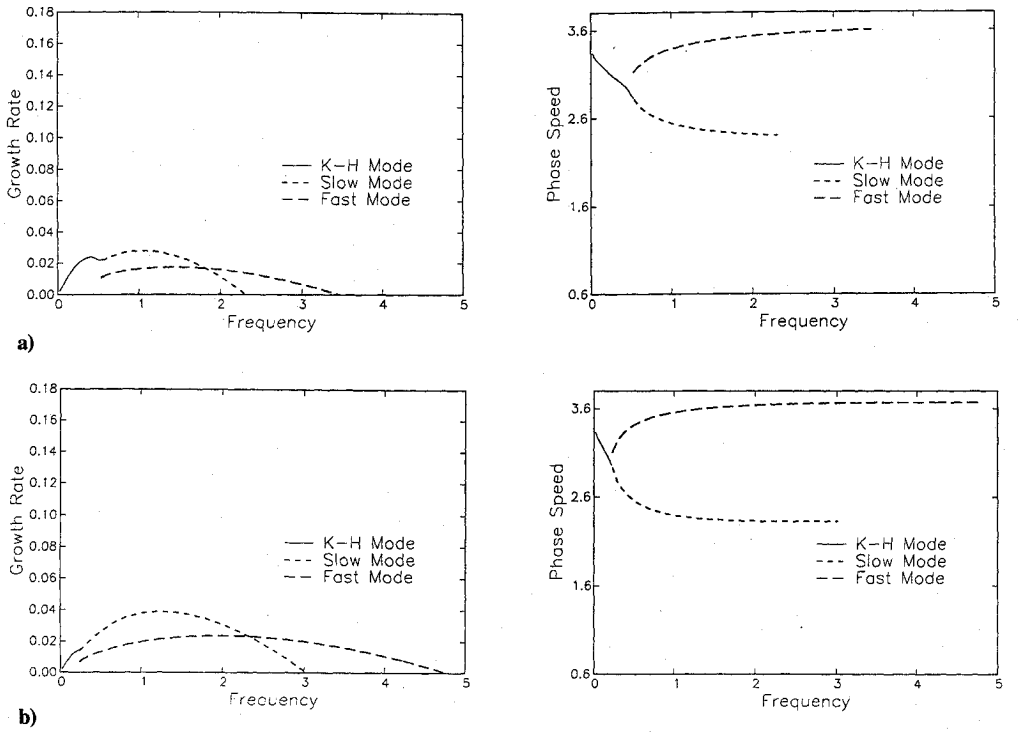

Fig. 6 Growth rate (left) and phase speed (right) vs frequency of Kelvin–Helmholtz and outer modes for a shear layer with $W = \delta = 0, \sigma = 1$: a) $T_r = 4$ and b) $T_r = 8$.

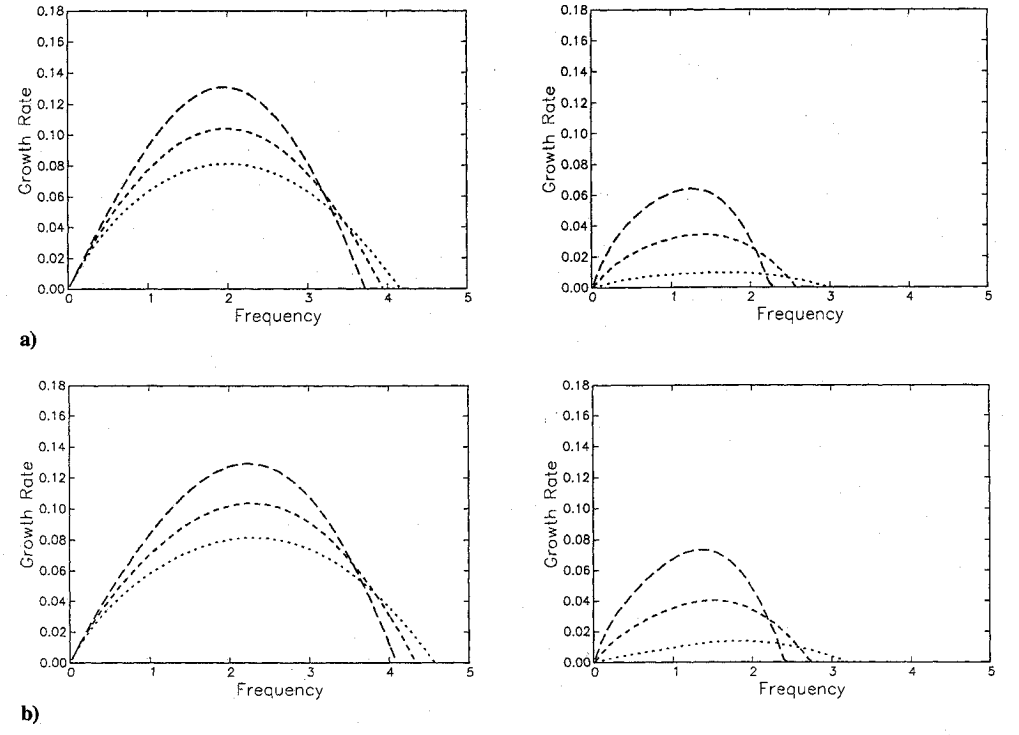

Fig. 7 Growth rate vs frequency for the Kelvin–Helmholtz (left) and wake modes (right) corresponding to velocity profiles with $\delta = 1$ and density profiles having $\sigma = 1$: a) $T_r = 4$ and b) $T_r = 8$.

profile at high-temperature ratio. In this case, three unstable modes are expected[12,17]: the Kelvin–Helmholtz mode, and two additional "outer" modes which appear due to density variation.

When more than a single mode is expected, distinction between the corresponding dispersion relations must be performed. In the present study, this exercise relies both on the methodology used in the determination of dispersion relations and on theoretical predictions regarding the asymptotic long-wave behavior of temporal modes.[17] As shown in Ref. 17, long waves are insensitive to density variation so that homogeneous flow predictions[22–24] regarding the corresponding temporal eigenvalues may be directly applied. Based on this knowledge, the analysis of Gaster[25] is then invoked to initialize the search of spatial dispersion relations. Thus, once their low-frequency "ends" are located, branches of the dispersion relation are extended by marching using small-frequency increments and applying the iterative procedure summarized in Sec. II. This approach enables us to easily distinguish between Kelvin–Helmholtz and wake modes. This is the case because these two modes have

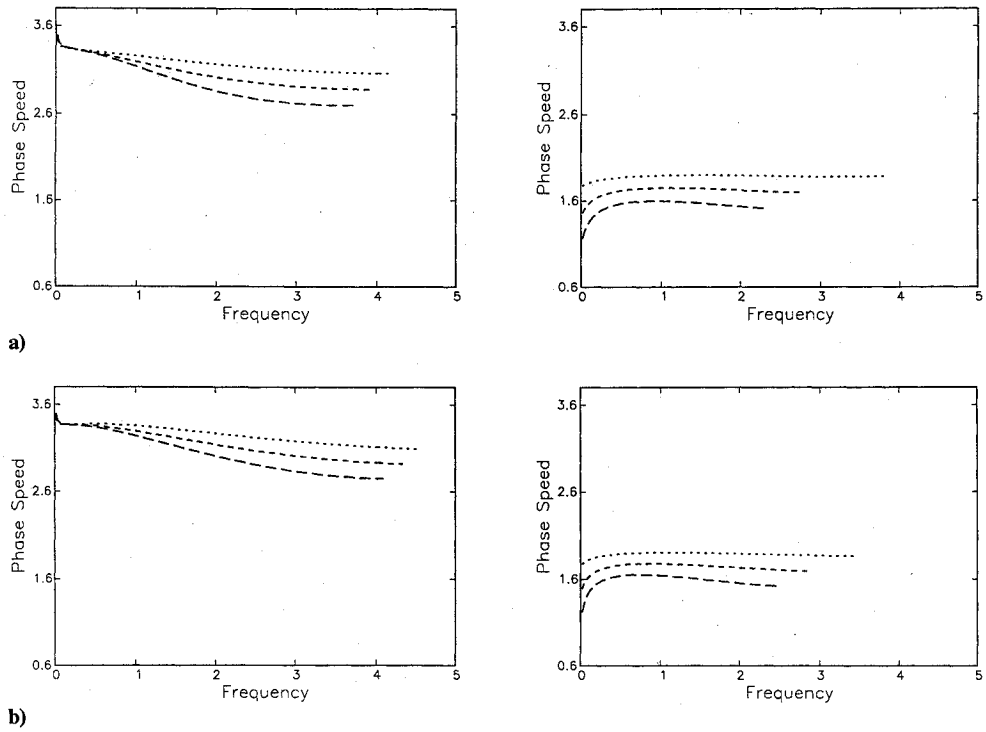

Fig. 8 Phase speed vs frequency for the Kelvin–Helmholtz (left) and wake modes (right) corresponding to velocity profiles with $\delta = 1$ and density profiles having $\sigma = 1$: a) $T_r = 4$ and b) $T_r = 8$.

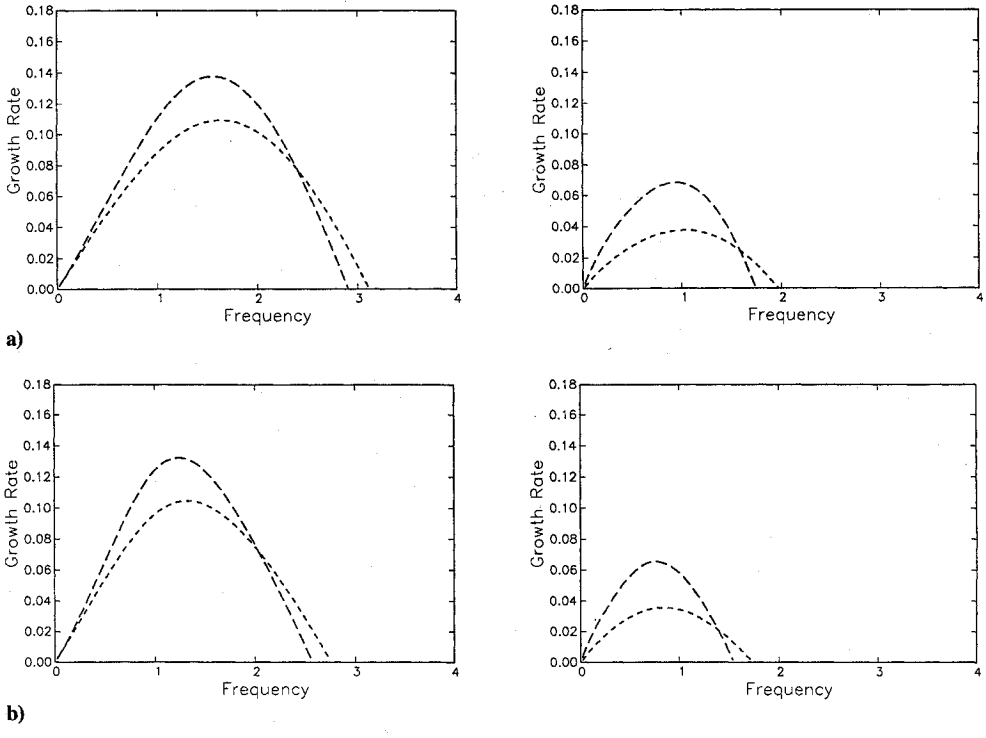

Fig. 9 Growth rate vs frequency for the Kelvin–Helmholtz (left) and wake modes (right) corresponding to velocity profiles with density profiles having $\sigma = 1$ and $T_r = 4$: a) $\delta = 2$ and b) $\delta = 3$.

distinct long-wave behavior and, at any given frequency, the corresponding eigenvalues remain well separated. Unfortunately, the same task is considerably more complicated when outer modes are present. Difficulties arise because long-wave asymptotics cannot be used to characterize the behavior of outer modes,[17] and because the corresponding dispersion relations may intersect that of the Kelvin–Helmholtz mode. This necessitates a more delicate analysis of the results, as summarized subsequently.

Analysis of stability results starts with a summary of homogeneous flow results. The latter are then contrasted with predictions for differentially heated layers having $\sigma = 1$. Next, the impact of varying σ is analyzed. Finally, illustration of the shape of unstable eigenfunctions is provided.

A. Homogeneous Flow

Linear stability predictions of the homogeneous flowfield ($T_r = 1$) are found in agreement with those of several previous studies, e.g., Refs. 1, 12, and the original analysis of Michalke.[26] Thus, to

Table 2 Selected configurations for flow visualization

Case	T_r	σ	W	δ	r	$-\alpha_i$	α_r	c	Perturbation
1	1	1	0	0	$\frac{1}{2}$	0.06425	0.443	1.33	KHM[a]
2	4	1	0	0	$\frac{1}{2}$	0.02783	0.415	1.05	SM[b]
3	4	1	0	0	$\frac{1}{2}$	0.01731	0.412	1.43	FM[c]
4[d]	4	1	0	0	$\frac{1}{2}$	0.02783	0.415	1.05	SM
						0.01731	0.412	1.43	FM
5	4	1.5	0	0	$\frac{1}{2}$	0.02424	0.147	0.44	KHM
6	1	1	0.75	1	$\frac{1}{2}$	0.1534	0.575	1.77	KHM
7	4	1	0.75	1	$\frac{1}{2}$	0.1307	0.680	0.95	KHM
8	1	1.5	0.75	1	$\frac{1}{2}$	0.0888	0.574	1.77	KHM

[a]KHM: Kelvin–Helmholtz mode. [b]SM: slow mode. [c]FM: fast mode. [d]Both modes combined.

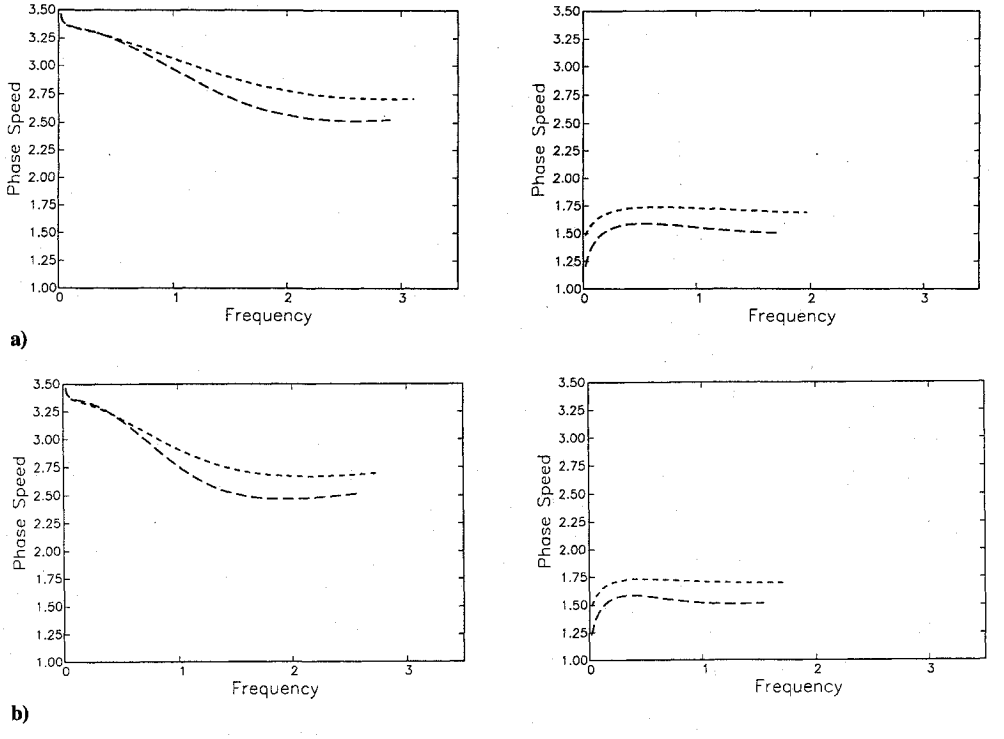

Fig. 10 Phase speed vs frequency for the Kelvin–Helmholtz (left) and wake modes (right) corresponding to velocity profiles with density profiles having $\sigma = 1$ and $T_r = 4$: a) $\delta = 2$ and b) $\delta = 3$.

later examine the impact of differential heating, we only present dispersion relations corresponding to the profiles of Fig. 2a (Figs. 4 and 5), and a brief summary of stability predictions.

As shown in Fig. 4, the maximum growth rates achieved by the Kelvin–Helmholtz mode are larger than those of the corresponding most unstable wake modes. This observation holds for all considered values of W. Increasing the profile thickness δ (not shown) results in a slight decrease in the growth rate of the most unstable Kelvin–Helmholtz mode and promotes the instability of wake modes. However, even at large δ, the Kelvin–Helmholtz mode is found dominant.

The presence of a wake deficit has a strong impact on the growth rate and phase speed of the dominant Kelvin–Helmholtz mode and small but noticeable effects on the most unstable frequency. As shown in Fig. 4, the maximum growth rate increases with increasing W; this is expected since higher wake deficits are characterized by higher vorticity concentrations. The phase speed of the dominant mode also exhibits a strong dependence on W; it is close to the mean flow velocity for the tanh profile and decreases steadily with increasing W (Fig. 5). On the other hand, the most unstable frequency is weakly dependent on W. Variation of the profile thickness δ (not shown) does not appear to have an important effect on the most unstable frequency or on the phase speed of the dominant mode.

B. Differentially Heated Flow

The impact of temperature ratio is first analyzed by varying T_r independently of the remaining flow parameters. Dispersion relations corresponding to the tanh profile are shown in Figs. 6 for $T_r = 4$ and 8. For the same temperature ratios, Figs. 7 and 8 depict dispersion relations for the nonmonotonic profiles having $\delta = 1$. Next, the impact of profile thickness is analyzed by considering a fixed temperature ratio $T_r = 4$ and velocity profiles with $\delta = 2$ and 3; results are plotted in Figs. 9 and 10, respectively.

Figures 6–10 immediately reveal that the response of the nonmonotonic layers to the imposed density variation is fundamentally different from that having $W = \delta = 0$. Consequently, results corresponding to the tanh profile are discussed separately.

Tanh Layer

When outer modes are expected, the determination of dispersion relations is performed in a stepwise fashion. As previously mentioned, the iterative search for eigenvalues corresponding to the tanh profile first starts by extending the low-frequency branch of the Kelvin–Helmholtz mode. Implementation of this procedure is complicated by the fact that the dispersion relation of the Kelvin–Helmholtz mode intersects that of one of the outer modes. When such an intersection occurs, the iterations subsequently converge toward the larger eigenvalue, namely, that of the relevant outer

mode. As a result, a single relation is obtained which partly corresponds to the Kelvin–Helmholtz mode and partly to one of the outer modes. Since the corresponding curve effectively captures the highest growth rates, we have not sought to extend individual branches toward their neutral stability limits. However, the location of the crossover between the two branches is always determined. As shown in Fig. 6, the location of the cross over between the two branches is characterized by a dramatic change in the behavior of the phase speed and is unambiguously determined based on the distinctive shape of the computed eigenfunction (see Sec. IV.D.). Once these branches are found, the dispersion relation for the remaining mode is determined by reinitializing the search near the crossover frequency.[17] Thus, in presenting the results, the dispersion relation of one of the outer modes appears as an extension of that of the Kelvin–Helmholtz mode; as a result, various branches are individually labeled.

Figure 6 shows that as the temperature ratio increases additional instability modes appear for the tanh layer. As already mentioned, these additional modes are associated with outer zeros of the function $U''+\rho'U'\rho$ and are, thus, called outer modes.[12] The outer mode having smaller phase speed is distinguished by higher growth rates than its counterpart; thus, the outer modes are also referred to as fast and slow modes.[1] At $T_r = 4$, the "combined" curve showing the Kelvin–Helmholtz and slow mode is distinguished by the appearance of two humps; at higher temperature ratio $T_r = 8$, the Kelvin–Helmholtz mode almost disappears.

Figure 6 also shows that as T_r increases the maximum growth rate of the Kelvin–Helmholtz mode decreases rapidly. Furthermore, the most unstable growth occurs at significantly smaller frequencies than in uniform density flow. Thus, the imposed differential heating of the flowfield leads to stabilization of the Kelvin–Helmholtz mode. This result is in agreement with the findings of Shin and Ferziger[12] and McMurtry et al.[13] who essentially reached the same conclusion.

As the Kelvin–Helmholtz mode is stabilized, the slow mode becomes dominant. Growth rate maximums for the Kelvin–Helmholtz and the dominant outer mode are comparable at $T_r = 4$, but the latter is noticeably higher at $T_r = 8$ where the Kelvin–Helmholtz mode is almost completely stabilized. Thus, for high-temperature ratios, the linear instability of the tanh layer is dominated by the amplification of the outer mode. Accordingly, the Kelvin–Helmholtz mode is not expected to contribute significantly to its early growth.

The observed behavior of the spatial outer modes admits similarities and differences to their temporal counterparts.[17] In both cases, the instability of the outer modes is promoted by higher values of the temperature ratio. In addition, as T_r increases, the bandwidth of the corresponding instability increases, and growth rate maximums occur at higher frequencies. However, in the temporal model, the outer modes are characterized by equal growth rate and wavelength and equal but opposite phase speed. Obviously, this symmetry is not recovered in the present study, as the spatial outer modes are distinguished by different frequencies, amplification rates, and phase speeds. Not surprisingly, it is the slow mode that assumes higher spatial growth factors and is, therefore, dominant.

Effect of Wake Deficit

Computed results for the nonmonotonic shear layers reveal a dramatically different response to the imposed heating of the flow. As previously mentioned, the appearance of additional instability modes does not occur for any of the nonmonotonic velocity profiles considered. Thus, as in the uniform-density case, flowfield instability is still governed by the dominant Kelvin–Helmholtz or wake mode. Unlike the tanh layer, no significant stabilization of the Kelvin–Helmholtz mode is detected for nonmonotonic layers (Figs. 7 and 9); the most unstable Kelvin–Helmholtz mode remains dominant, as is the case in homogeneous flow.

However, the imposition of a non uniform-density field still has noticeable effects on the characteristics of the dominant mode. In particular, the imposed heating results in a widening of the instability bandwidth of the Kelvin–Helmholtz mode. For thin velocity profile ($\delta = 1$), this phenomenon is accompanied by an increase in the frequency and phase speed of the most unstable mode (Figs. 7 and 8). In addition, the maximum amplification factors (Fig. 7) decrease slightly with increasing temperature ratio. These effects are substantially attenuated when the flow profile is thick ($\delta = 2$ or 3, Figs. 9 and 10), in which case the stability characteristics of the flow appear to be weakly sensitive to the imposed heating.

The predicted response of the spatially developing nonmonotonic layers differs slightly from its temporal counterpart.[17] In the latter case, the stability bandwidth and amplification curves are found almost insensitive to the imposed density distribution, whose impact is restricted to weak modulation of the phase speed of the unstable waves. In both cases, however, the effects of imposed heating are far less pronounced than for the tanh profile.

C. Effect of Density Profile Thickness

The impact of density profile thickness on flowfield stability is analyzed by fixing $T_r = 4$ and considering three additional values $\sigma = 0.5, 0.75$, and 1.5. Amplification curves corresponding to the tanh profile are shown in Fig. 11, and are contrasted with results for profiles having $\delta = 1$ (Fig. 12). For brevity, dispersion relations for the velocity profile with the smallest wake deficit are omitted.

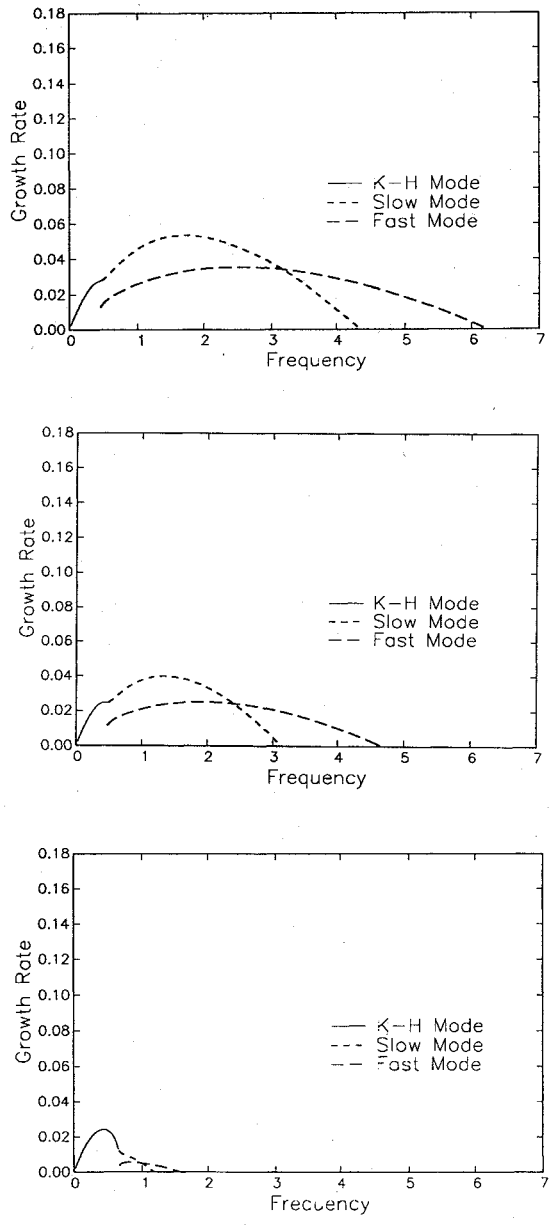

Fig. 11 Growth rate vs frequency of Kelvin–Helmholtz and outer modes for a shear layer with $W = \delta = 0$, $T_r = 4$: a) $\sigma = 0.5$, b) $\sigma = 0.75$, and c) $\sigma = 1.5$.

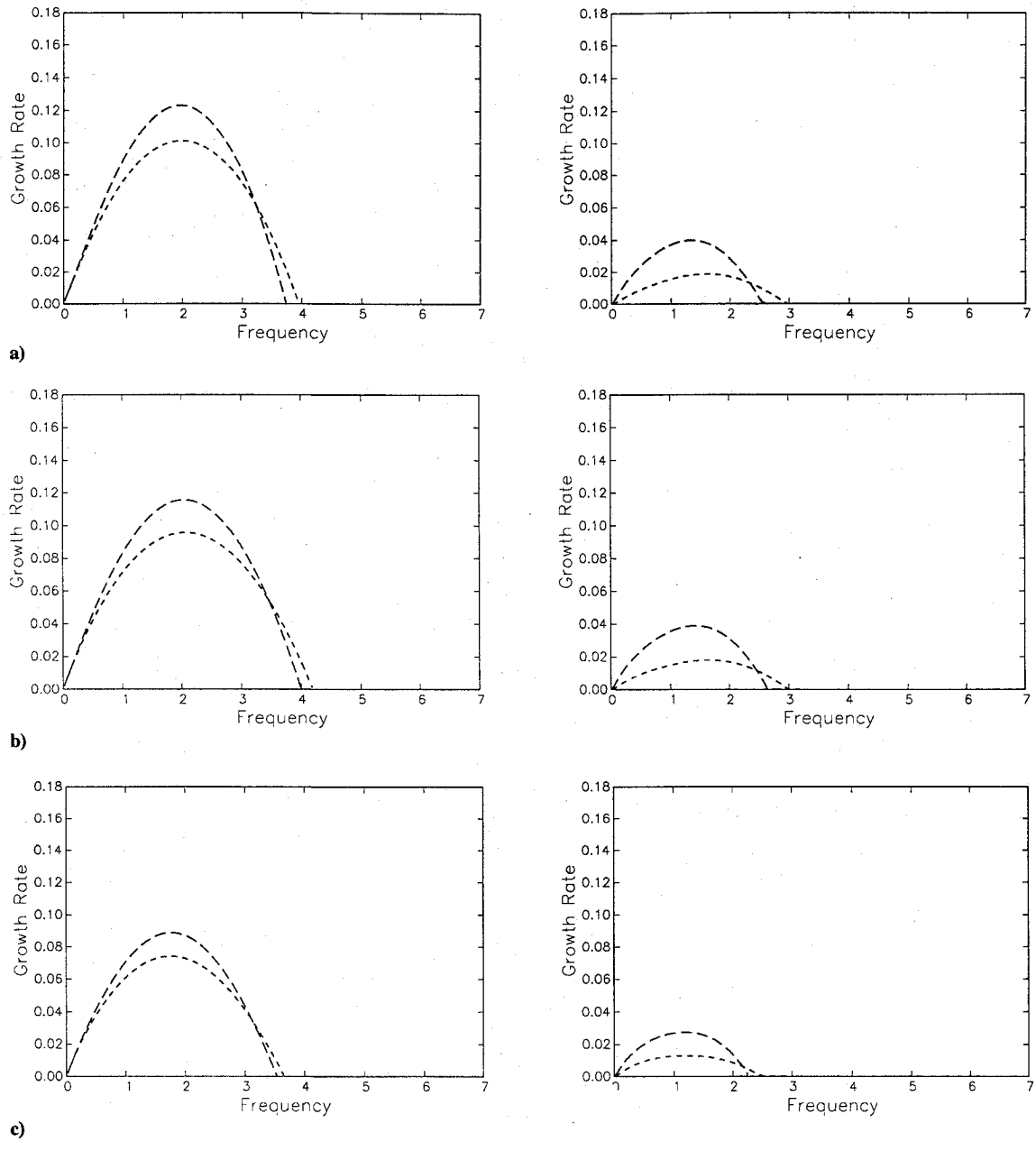

Fig. 12 Growth rate vs frequency for the Kelvin–Helmholtz (left) and wake modes (right) corresponding to velocity profiles with $\delta = 1$ and density profiles having $T_r = 4$, curve corresponding to the smallest wake deficit is omitted): a) $\sigma = 0.5$, b) $\sigma = 0.75$, and c) $\sigma = 1.5$.

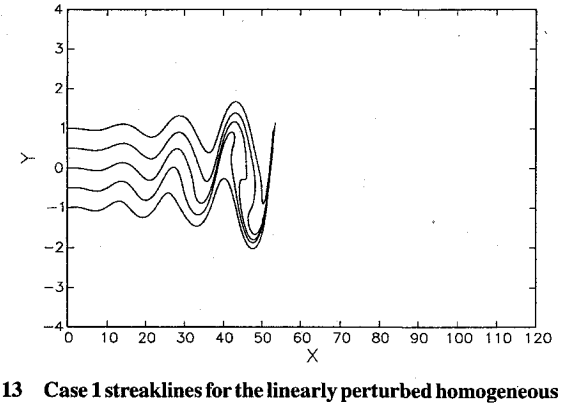

Fig. 13 Case 1 streaklines for the linearly perturbed homogeneous tanh layer.

As shown in Fig. 11, the stability of the tanh layer is strongly dependent on σ. Decreasing σ below unity results in an increase in the stability bandwidths and maximum growth rates of both outer modes. This behavior is accompanied by a considerable increase in the frequency of the dominant outer mode; for $\sigma = 0.5$, the most unstable frequency is approximately twice that of most unstable homogeneous Kelvin–Helmholtz mode. However, the Kelvin–Helmholtz mode is further stabilized. Thus, the decrease of the heated zone thickness promotes the instability of the outer modes and further inhibits the growth of the Kelvin–Helmholtz mode.

Examination of results obtained at $\sigma = 1.5$ indicates that the trends are reversed if the density thickness increases. Figures 11 show that increasing σ promotes the instability of the Kelvin–Helmholtz mode, whose maximum spatial growth rate approaches that established in homogeneous flow. Meanwhile, both the instability bandwidth and growth rates of the outer modes are substantially reduced, and flowfield instability is now dominated by that of the Kelvin–Helmholtz mode. This trend is expected to persist if σ is increased even further; in the limit $\sigma \to \infty$, the entire vorticity layer would be lie in a uniformly heated region, in which case the outer modes would not appear and homogeneous flow predictions would be recovered.

Nonmonotonic shear layers exhibit a weak response to the details of the imposed density profile. For thin velocity profile ($\delta = 1$), Fig. 12 indicates that near unity σ values lead to a small decrease in

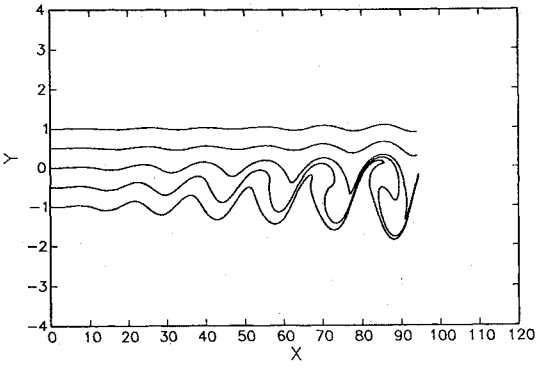

a) Case 2

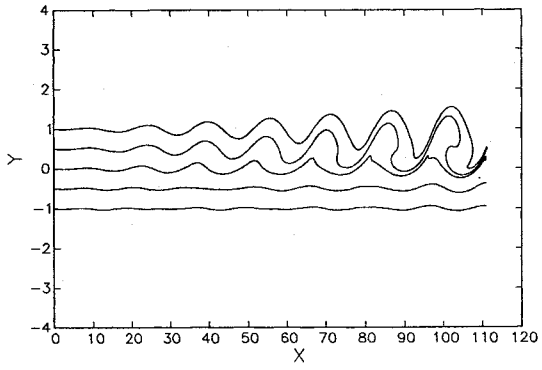

b) Case 3

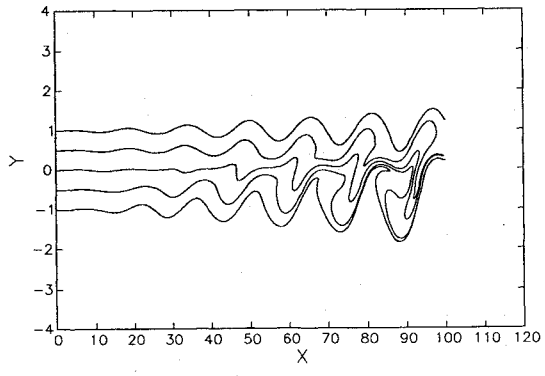

c) Case 4

Fig. 14 Streaklines for the linearly perturbed tanh layer, plots correspond to the unstable outer modes of cases 2–4 in Table 2, respectively, arranged from top.

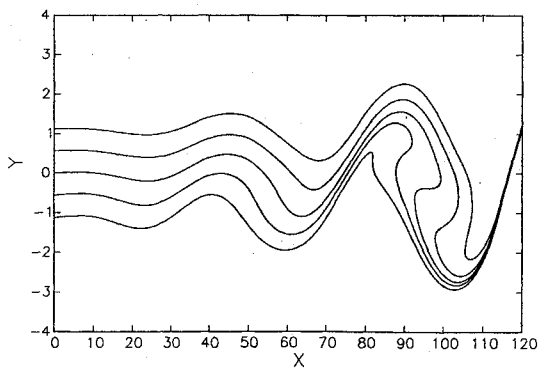

Fig. 15 Streaklines for the tanh layer, linearly perturbed with the unstable mode Kelvin–Helmholtz mode of case 5 in Table 2.

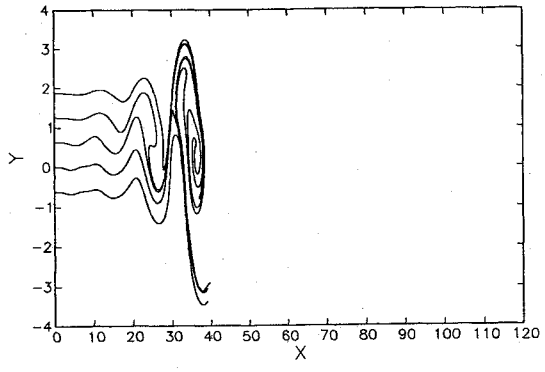

a) Case 6

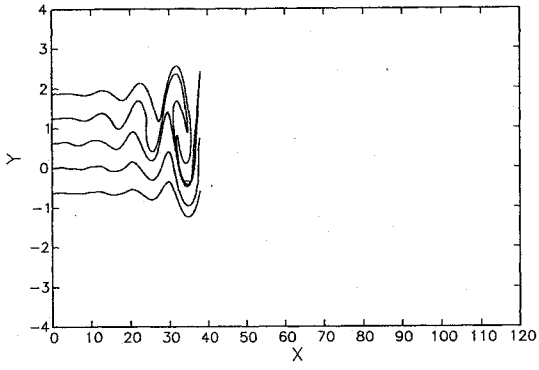

b) Case 7

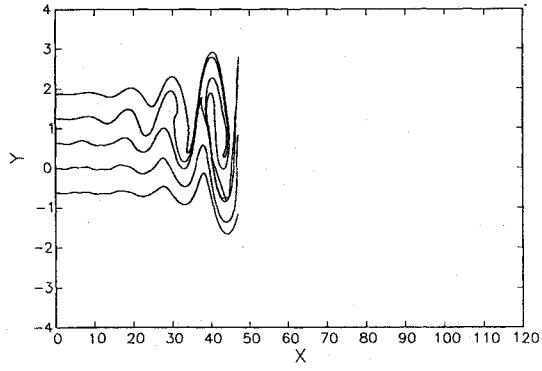

c) Case 8

Fig. 16 Streaklines for the linearly perturbed layer with $W = 0.75$ and $\delta = 1$, plots correspond to the unstable Kelvin–Helmholtz modes of cases 6–8 in Table 2, respectively, arranged from top.

the most unstable growth rate of the Kelvin–Helmholtz mode and to small modulation of the instability bandwidth and of the most unstable frequency. For thick velocity profiles ($\delta = 2$ and 3) the instability of the Kelvin–Helmholtz mode is almost insensitive to σ; the results are, thus, omitted.

D. Visualization of Unstable Eigenfunctions

Visualization of the unstable eigenfunctions is provided by plotting streaklines of the linearly perturbed flowfield.[1] The streaklines are computed by continuously releasing material particles, whose locations are updated by integrating the equation of motion,

$$\frac{\mathrm{d}\boldsymbol{x}}{\mathrm{d}t} = \boldsymbol{U}_m(y) + \varepsilon\,\mathrm{Re}\left[\sum_{j=1}^{L} \nabla \times \Psi_j(x, y, t)\right] \tag{6}$$

where $\boldsymbol{U}_m(y)$ is the mean flow velocity, $\Psi_j(x, y, t) = \psi_j(y) \exp[i(\alpha_j x - \beta_j t)]$ is the disturbance stream function, and $L = 1, 2$ according to whether one or two unstable modes are present. The disturbance stream function is normalized so that the maximum

disturbance velocity has unit magnitude, whereas $\varepsilon = 0.02$ in all calculations.

The growth of unstable eigenfunctions is illustrated for eight cases (Table 2), whose selection aims at highlighting differences in the response of monotonic and nonmonotonic layers to the imposed density variation. The first five cases of Table 2 consider a tanh layer, whereas the remaining three focus on a nonmonotonic layer with $W = 0.75$ and $\delta = 1$. We start by considering the dominant Kelvin–Helmholtz mode in a homogeneous field (cases 1 and 6). Next, we focus our attention on a differentially heated flow with $T_r = 4$ and $\sigma = 1$; for the tanh layer, cases 2–4 correspond to the slow mode, the fast mode, and both outer modes combined, respectively, whereas case 7 represents the dominant Kelvin–Helmholtz mode of the nonmonotonic layer. Finally, the effect of thickening the density profile is examined. The dominant Kelvin–Helmholtz mode in a heterogeneous field with $T_r = 4$ and $\sigma = 1.5$ is selected in cases 5 and 8 for the tanh and nonmonotonic profiles, respectively. Streaklines of the linearly perturbed field are plotted in Figs. 13–16, which illustrate the amplification of the unstable modes of case 1, cases 2–4, case 5, and cases 6–8, respectively.

For a homogeneous field, the computed spatial deformation of the streaklines is reminiscent of Kelvin–Helmholtz vortices which form following the nonlinear wave breaking of unstable modes. Although the linearized unsteady flowfield used to generate these streaklines does not yield a realistic illustration of the rollup of the layer, the streakline pattern may still be used to obtain a qualitative picture of the impact of finite wave growth. In particular, the locations where negative particle velocities first occur may be used as a measure of spatial amplification rates and to distinguish the various cases considered.

When a differentially heated field with $T_r = 4$ and $\sigma = 1.0$ is considered, the Kelvin–Helmholtz mode is no longer dominant, and the instability of the tanh layer is governed by the growth of outer modes. As shown in Fig. 14, the latter yield a distinctively different flow structure from the previous case. Whereas the dominant slow mode primarily affects the low-speed stream, the fast mode amplifies primarily on the high-speed side of the layer. Individual growth of the outer modes results in streakline deformation which slightly resembles that observed in homogeneous flow. When both outer modes develop simultaneously, the structure of the deformed streaklines resembles more the evolution of a thin wake than a spatially developing layer, although the (frozen) mean flow is given by a monotonic profile. This behavior is qualitatively similar to that observed in direct simulations of temporal outer modes,[17] which show the formation of weak incoherent eddies. However, it should be emphasized that temporal simulations[17] also indicate that temporal outer modes tend to saturate rapidly and that nonlinear growth of these modes does not lead to substantial deformation of the flow. Thus, the qualitative flow structure predicted by the streaklines of the linearly perturbed flow may not be simply extrapolated. Consequently, the impact of outer mode amplification on nonlinear evolution of the differentially heated flow should be further analyzed using the full equations of motion.

For a thick density profile, $\sigma = 1.5$, linear stability predictions show that the Kelvin–Helmholtz mode is once again dominant. However, the associated growth rate is smaller than that of the most unstable mode in a homogeneous field. The stabilization of the Kelvin–Helmholtz mode due to the heating of the flowfield is reflected in Fig. 15, which shows that the spatial deformation of the streamlines, although similar to that observed in a homogeneous field, occurs at a smaller rate. In particular, particle velocity reversal is first detected at a much larger downstream distance. Streaklines of the nonmonotonic velocity profile (Fig. 16) also reflect the results of the linear stability calculations. The predicted weak response of the flowfield to the imposed form of differential heating is manifested by similar streakline structures and by the weak dependence of the predictions on the details of the density distribution.

V. Conclusions

In this work, the inviscid linear spatial instability of two-dimensional, heterogeneous, monotonic and nonmonotonic shear layers is analyzed. The initial velocity profiles are prescribed by superposing a wake component on the familiar tanh shear layer profile. The initial density field corresponds to a Gaussian temperature spike, used to model the development of a nonpremixed reaction. Unstable mode characteristics are interpreted in terms of five independent parameters: the velocity ratio, the wake deficit, the thicknesses of the velocity and density profiles, and the temperature ratio. Computed results show that the stability properties of the tanh (nonmonotonic) layer are strongly (weakly) sensitive to the imposed heating; predictions for monotonic and nonmonotonic profiles are summarized separately as follows.

Tanh Layer

As the temperature ratio increases, stabilization of the Kelvin–Helmholtz mode occurs. The stabilization process is associated with a decrease in the frequency and amplitude of the most unstable mode and in its overall stability bandwidth. The generation of two unstable outer modes (fast and slow modes) is observed. The latter are characterized by a wide instability bandwidth and achieve their maximum growth at substantially higher frequencies than that of the most unstable homogeneous Kelvin–Helmholtz mode. For high-temperature ratio, the instability of the layer is dominated by that of the slow mode. However, this trend is reversed if the thickness of the heated zone is increased. In this case, the Kelvin–Helmholtz mode is once again dominant, as the instability of the outer modes is inhibited. On the other hand, thinning of the density profile thickness promotes (inhibits) the instability of outer (Kelvin–Helmholtz) modes.

Visualization of eigenfunctions of outer modes reveals that these lead to radically different structures than those expected from homogeneous flow predictions. In particular, the impact of outer mode growth appears to be localized near the critical point of the corresponding eigenfunction. When both linear modes amplify simultaneously, results show the formation of weak structures that resemble more a wake than a shear layer.

Finally, it is emphasized that linear stability predictions of the outer mode behavior should not be simply extrapolated to nonlinearly evolving flow. Previous nonlinear simulations of the evolution of temporal outer modes indicate that these tend to saturate rapidly and result in weak incoherent vortical structures.[17] Thus, although spatial linear stability predictions indicate that outer modes can achieve large amplification rates, it is as yet hard to fully assess their impact on nonlinear flowfield evolution. This issue will be tackled in a future study.

Effect of Wake Deficit

Nonmonotonic shear layers appear to be weakly sensitive to the imposed form of differential heating. In particular, no significant stabilization of the Kelvin–Helmholtz mode is observed, and the latter is found dominant in all cases considered. For large wake profile thickness, the properties of the dominant Kelvin–Helmholtz mode are almost insensitive to the details of the density distribution. For thin wake profile thickness, increasing the temperature ratio leads to small increase in the frequency of the most unstable Kelvin–Helmholtz mode and a small decrease in its growth rate. Variation of the thickness of the density profile does not appear to have a major impact on stability predictions.

The observed differences in linear stability behavior of differentially-heated monotonic and nonmonotonic layers bear important implications concerning flowfield modeling. In particular, the present predictions indicate that the modeling of shear layers as initial velocity discontinuities or monotonically increasing velocity profiles may not always be justified. Although this issue does not appear to be important in homogeneous flow applications, the presence of zones of large density variations may require a more delicate treatment and more elaborate flowfield modeling.

Temporal Models and Nonpremixed Flames

Temporal shear layer models have been frequently used to study the dynamics of both homogeneous and reacting shear flows. Implementation of such models typically relies on an appropriately translating reference frame and on simplified boundary conditions.

Using this approach, good predictions are typically obtained regarding the wavelengths and frequencies of unstable modes and of their impact on the flow structure. Despite their inability to yield accurate predictions regarding the spatial growth of the layers[3] and the fine details of the vortical structures which form due to nonlinear wave growth and wave breaking,[26,27] temporal models often constitute efficient means to isolate the essential dynamics of a large number of free shear flows.

The observed similarities in the response of temporal and spatial layers—both monotonic and nonmonotonic—to the presently imposed mode of differential heating indicate that the temporal model will share most of the properties established for homogeneous flow. However, it should be emphasized that the application of the temporal model to analyze the response of reacting shear layers to the heating mechanisms is extremely complicated when monotonic shear layers are considered. In addition to the limitations just mentioned, one is faced with additional difficulties which are associated with the dependence of unstable wave numbers and frequencies to the details of the prevailing density distribution. Thus, the study of the impact of heat deposition cannot be performed independently of wavelengths, especially if long-time simulations are targeted during which the density field changes significantly. The consideration of nonmonotonic shear layers provides a simple means to overcome these difficulties,[28] since most unstable wavelengths and frequencies are weakly sensitive to the details of the density distribution.

References

[1]Koochesfahani, M. M., and Frieler, C. E., "Instability of Nonuniform Density Free Shear Layers with a Wake Profile," *AIAA Journal*, Vol. 27, No. 12, 1989, pp. 1735–1740.

[2]Yu, M.-H., and Monkewitz, P. A., "The Effect of Nonuniform Density on the Absolute Instability of Two-Dimensional Inertial Jets and Wakes," *Physics of Fluids A*, Vol. 2, No. 7, 1990, pp. 1175–1181.

[3]Dimotakis, P. E., "Turbulent Free Shear Layer Mixing," AIAA Paper 89-0262, Jan. 1989.

[4]Brown, G. L., and Roshko, A., "On Density Effects and Large Structure in Turbulent Mixing Layers," *Journal of Fluid Mechanics*, Vol. 64, Pt. 4, July 1974, pp. 775–816.

[5]Maslowe, S. A., and Kelly, R. E., "Inviscid Instability of an Unbounded Heterogeneous Shear Layer," *Journal of Fluid Mechanics*, Vol. 48, Pt. 2, July 1971, pp. 405–415.

[6]Koop, C. G., and Browand, F. K., "Instability and Turbulence in Stratified Fluid with Shear," *Journal of Fluid Mechanics*, Vol. 93, Pt. 1, July 1979, pp. 135–159.

[7]Huerre, P., and Monkewitz, P. A., "Local and Global Instabilities in Spatially Developing Flows," *Annual Review of Fluid Mechanics*, Vol. 22, 1990, pp. 473–537.

[8]Monkewitz, P. A., and Sohn, K. D., "Absolute Instability in Hot Jets," *AIAA Journal*, Vol. 26, No. 8, 1988, pp. 911–916.

[9]Huerre, P., and Monkewitz, P. A., "Absolute and Convective Instabilities in Free Shear Layers," *Journal of Fluid Mechanics*, Vol. 159, 1985, p. 151.

[10]Jackson, T. L., and Grosch, C. E., "Inviscid Spatial Stability of a Compressible Mixing Layer. Part 2. The Flame Sheet Model," *Journal of Fluid Mechanics*, Vol. 217, Aug. 1990, pp. 391–420.

[11]Hu, F. Q., Jackson, T. L., Lasseigne, D. G., and Grosch, C. E., "Absolute-Convective Instabilities and Their Associated Wave Packets in a Compressible Reacting Layer," *Physics of Fluids A*, Vol. 5, No. 4, 1993, pp. 901–915.

[12]Shin, D. S., and Ferziger, J. H., "Linear Stability of the Reacting Mixing Layer," *AIAA Journal*, Vol. 29, No. 10, 1991, pp. 1634–1642.

[13]McMurtry, P. A., Riley, J. J., and Metcalfe, R. W., "Effects of Heat Release on the Large-Scale Structure in Turbulent Mixing Layers," *Journal of Fluid Mechanics*, Vol. 199, Feb. 1989, pp. 297–332.

[14]Hegde, U. G., and Zinn, B. T., "Vortical Mode Instability of Shear Layers with Temperature and Density Gradients," *AIAA Journal*, Vol. 28, No. 8, 1990, pp. 1389–1396.

[15]Krishnan, A., "Numerical Study of Vorticity-Combustion Interactions in Shear Flow," Ph.D. Thesis, Dept. of Mechanical Engineering, Massachusetts Inst. of Technology, Cambridge, MA, May 1989.

[16]Ghoniem, A. F., and Krishnan, A., "Origin and Manifestation of Flow-Combustion Interactions in a Premixed Shear Layer," *Twenty-Second Symposium (International) on Combustion*, Combustion Inst., Pittsburgh, PA, 1988, pp. 665–675.

[17]Knio, O. M., and Ghoniem, A. F., "Stability of Differentially Heated Shear Layers," *Vortex Flows and Related Numerical Methods*, edited by J. T. Beale, G.-H. Cottet, and S. Huberson, Kluwer, Academic, Norwell, MA, 1993, pp. 341–372.

[18]Lang, D. B., "Laser Dopler Velocity and Vorticity Measurements in Turbulent Shear Layers," Ph.D. Thesis, Dept. of Mechanical Engineering, California Inst. of Technology, Pasadena, CA, May 1985.

[19]Dimotakis, P. E., and Miake-Lye, R. C., and Papantoniou, D. A., "Structure and Dynamics of Round Turbulent Jets," *Physics of Fluids*, Vol. 26, No. 11, 1993, pp. 3185–3192.

[20]Betchov, R., and Criminale, W. O., *Stability of Parallel Flows*, Academic, New York, 1967, Chap. 3.

[21]Koch, W., "Local Instability Characteristics and Frequency Determination of Self-Excited Wake Flows," *Journal of Sound and Vibration*, Vol. 99, No. 1, 1985, pp. 53–83.

[22]Drazin, P. G., and Howard, L. N., "Hydrodynamic Stability of Parallel Flow of Inviscid Fluid," *Advances in Applied Mechanics*, Vol. 9, May 1966, pp. 1–89.

[23]Drazin, P. G., and Reid, W. H., *Hydrodynamic Stability*, Cambridge Univ. Press, New York, 1981, Chap. 3.

[24]Drazin, P. G., and Howard, L. N., "The Instability to Long Waves of Unbounded Parallel Inviscid Flow," *Journal of Fluid Mechanics*, Vol. 14, Pt. 2, Oct. 1962, pp. 257–283.

[25]Gaster, M., "A Note on the Relation Between Temporally-Increasing and Spatially-Increasing Disturbances in Hydrodynamic Stability," *Journal of Fluid Mechanics*, Vol. 14, Pt. 2, Oct. 1962, pp. 222–224.

[26]Michalke, A., "On Spatially Growing Disturbances in an Inviscid Shear Layer," *Journal of Fluid Mechanics*, Vol. 23, Pt. 3, Nov. 1965, pp. 521–544.

[27]Dimotakis, P. E., "Two-Dimensional Shear-Layer Entrainment," *AIAA Journal*, Vol. 24, No. 11, 1986, pp. 1791–1796.

[28]Knio, O. M., Shi, X., and Ghoniem, A. F., "Lagrangian Simulation of Flamelet Combustion," AIAA Paper 93-0247, Jan. 1993.